

Assessing Polymer Phase Behavior in Explicit Solvent and with Vacancies

Davide Marcato*

Scuola Internazionale Superiore di Studi Avanzati (SISSA), Via Bonomea 265, 34136 Trieste, Italy

Achille Giacometti†

*Dipartimento di Scienze Molecolari e Nanosistemi,
Università Ca' Foscari Venezia, 30123 Venezia, Italy and
European Centre for Living Technology (ECLT) Ca' Bottacin,
3911 Dorsoduro Calle Crosera, 30123 Venezia, Italy*

Amos Maritan‡

*Laboratory of Interdisciplinary Physics, Department of Physics and Astronomy “G. Galilei”,
University of Padova, Padova, Italy and INFN, Sezione di Padova, via Marzolo 8, 35131 Padova, Italy*

Angelo Rosa§

Scuola Internazionale Superiore di Studi Avanzati (SISSA), Via Bonomea 265, 34136 Trieste, Italy

(Dated: July 3, 2024)

We present a lattice model for polymer solutions, explicitly incorporating interactions with solvent molecules and the contribution of vacancies. By exploiting the well-known analogy between polymer systems and the $O(n)$ -vector spin model in the limit $n \rightarrow 0$, we derive an exact field-theoretic expression for the partition function of the system. The latter is then evaluated at the saddle-point, providing a mean-field estimate of the free energy. The resulting expression, which conforms to the Flory-Huggins type, is then used to analyze the system’s stability with respect to phase separation, complemented by a numerical approach based on convex hull evaluation. We demonstrate that this simple lattice model can effectively explain the behavior of polymer systems in explicit solvent, which has been predominantly investigated through numerical simulations. This includes both single-chain systems and polymer solutions. Our findings emphasize the fundamental role of vacancies whose presence, rendering the system a ternary mixture, is a crucial factor in the observed phase behavior.

Introduction – In phase transitions for multi-component systems [1–3], the study of polymer chains in a bath of solvent molecules occupies a special place [4–9]. Take, for instance, a single chain in the infinite-dilution limit: upon changing from “good” to “poor” solvent conditions, the polymer undergoes a drastic change in size, from a random coil to a globular collapsed conformation, the analogue of the gas-liquid transition. In polymer solutions, with each chain simultaneously interacting with both the solvent and the other chains, an even richer hierarchy of ordered structures appears upon cooling [10, 11]. Within this framework, in past years extensive numerical work was dedicated [12–17] to explore the interplay between the distinct interactions (monomer-monomer (mm) vs. monomer-solvent (ms) vs. solvent-solvent (ss)) behind chains’ swelling and collapse. In a recent interesting study [16], the authors used model Lennard-Jones polymer chains in *explicit* solvent of moderate density to profile polymer/solvent phase separation when ms affinity competes with mm and ss ones. Their work unveiled unexpected *re-entrant* polymer collapse for *strong* ms affinity (Fig. S1(a) in Supplemental Material

(SM [18])), absent in *implicit* solvent simulations, that was ascribed to the effective mm attraction “bridged” by the solvent (a quite similar phenomenon holds in the colloidal realm [19]). A later study [17], for a single chain and much *lower* solvent density, confirmed this result for a wider parameter space (Fig. S1(b) in SM [18]).

In this complex scenario, there is significant quest for theoretical models that would assist both in interpreting numerical experiments and in the systematic exploration of parameter space. Motivated by these considerations, in this Letter we introduce a novel $O(n)$ -vector spin model for polymer solutions on the d -dimensional hypercubic lattice that integrates the explicit roles of both solvent and vacancies, and solve it within a mean-field (MF) approximation. Then, we show how the MF theory (i) reproduces several phenomenological Flory-Huggins free energies [20, 21] in the appropriate limits and (ii) combined with a convenient graphical convex hull scheme, recapitulates and rationalizes the aforementioned numerical results as well as “polymer-assisted condensation” [22], a molecular mechanism involved in the nucleation of biomolecular condensates [23–25].

Microscopic model and Flory-Huggins free energy – Our approach rests on the well-known mapping between polymer systems and the formal $n \rightarrow 0$ limit of the $O(n)$ -vector model for interacting spins on the hypercubic lattice in d spatial dimensions [26–31]. Polymer chains and solvent molecules are arranged on the lattice of total sites

* dmarcato@sissa.it

† achille.giacometti@unive.it

‡ amos.maritan@unipd.it

§ anrosa@sissa.it

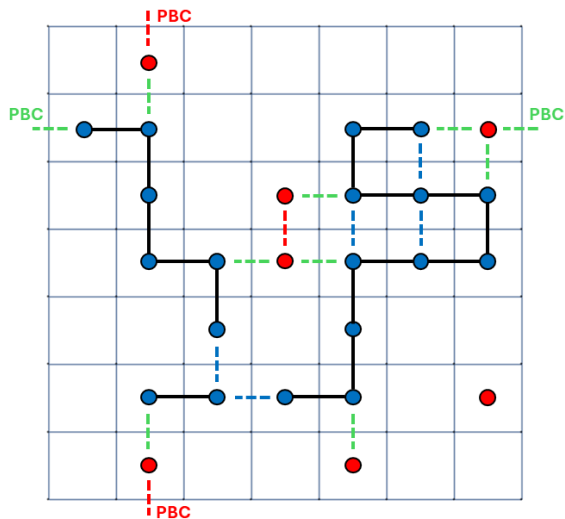


FIG. 1. Illustration of a particular configuration on the square lattice ($d = 2$), with $N = 7 \times 7 = 49$ sites. Monomers and the bonds joining them into polymer chains are represented, respectively, by blue dots and solid black lines, while solvent molecules are represented by red dots. Dashed lines are for nearest-neighbour interactions: different colors distinguish between mm pairs (blue), ss pairs (red) and ms pairs (green). In the example here (Eq. (1)): $N_c = 3$, $N_b = 16$, $N_s = 7$ and $N_{mm} = 5$, $N_{ss} = 2$, $N_{ms} = 9$ (notice also pair interactions *via* periodic boundary conditions (PBC)).

N (Fig. 1), with the lattice step as our unit of length. Excluded volume interactions are strictly enforced: so a lattice site can be occupied by either a monomer, or a solvent molecule, or a vacancy (*i.e.*, it is empty). For convenience [31] we adopt the *grand canonical* ensemble, with non-fixed total number of polymer chains N_c , bonds N_b and solvent molecules N_s (as a consequence, the system is typically *polydisperse*) and whose mean values depend on respective fugacities κ_c , κ_b and κ_s [32]. Then, with $\beta = 1/(k_B T)$ the Boltzmann factor at temperature T (k_B is the Boltzmann constant), the grand canonical partition function of the system reads

$$Z = \sum_{\{C\}} \kappa_c^{N_c} \kappa_b^{N_b} \kappa_s^{N_s} e^{-\beta(\epsilon_{mm} N_{mm} + \epsilon_{ss} N_{ss} + \epsilon_{ms} N_{ms})}, \quad (1)$$

where the sum is for all possible configurations $\{C\}$, and N_{mm} , N_{ss} and N_{ms} are, respectively, the total number of non-bonded mm , ss and ms pairs sitting at nearest-neighbor lattice positions (including periodic boundary conditions, Fig. 1) with corresponding pair interactions ϵ_{mm} , ϵ_{ss} and ϵ_{ms} (so setting the stage for modeling the systems of Refs. [16, 17], see also Fig. S1 in SM [18]).

In the $n \rightarrow 0$ limit, the partition function (1) can be recast in a convenient field-theoretic form (details in Sec. S1 A in SM [18]) that, although mathematically intractable, is particularly amenable to a systematic expansion around the saddle-point [28–31]. By taking only the leading term of the expansion (equivalent to the MF approximation, Sec. S1 B in SM [18], in particular

Eq. (S19)), we get a simple expression for the *grand potential* per site, $\beta\Omega \equiv -\ln(Z)/N$ that, by a Legendre transform (Sec. S1 C in SM [18]), gives the final system MF free energy per site,

$$\begin{aligned} \beta f(\phi_m, \phi_s, \ell) = & d\beta\epsilon_{mm}\phi_m^2 + d\beta\epsilon_{ss}\phi_s^2 + 2d\beta\epsilon_{ms}\phi_m\phi_s \\ & + (1 - \phi_m - \phi_s)\ln(1 - \phi_m - \phi_s) \\ & + \frac{\phi_m}{\ell}\ln(\phi_m) + \phi_s\ln(\phi_s) \\ & + \phi_m\ln\left(\frac{(1 - 2/\ell)^{1-2/\ell}(2/\ell^2)^{1/\ell}}{(2d e^{\beta\epsilon_{mm}})^{-1}(1 - 1/\ell)^{1-1/\ell}}\right), \end{aligned} \quad (2)$$

as a function of monomer density (ϕ_m), solvent density (ϕ_s) and *mean* chain contour length (ℓ) (all experimentally accessible quantities).

Interestingly, βf is of the Flory-Huggins form [20, 21, 33]. However, unlike most conventional presentations (for instance, see [2]), the derivation of (2) proceeds from a genuinely microscopic model (Eq. (1)) and it can be always expanded beyond the saddle-point by the systematic inclusion of higher-order corrections [34]. From the physical point of view, βf (2) describes the thermodynamics of a *ternary* mixture [35, 36] of polymers, solvent and vacancies, with the constraint $\phi_m + \phi_s + \phi_v = 1$ where ϕ_v is the vacancy density; it reduces to known cases of *binary* mixtures when one species is absent (Sec. S1 C in SM [18]). Importantly, the ratio ϕ_m/ℓ tunes the chain number density: at fixed ϕ_m and in the thermodynamic limit $N \rightarrow \infty$, a finite ℓ corresponds to a (polydisperse) multi-chain solution, while $\ell \rightarrow \infty$ gives the single-chain limit [37]. Eq. (2) is therefore valid for both single and multiple chains, as it will be discussed further below and in SM [18].

Single-chain systems: two-phase stability – From a thermodynamic perspective, the polymer coil state corresponds to a stable mixed phase whereas the globule state is a phase-separate system where one phase has $\phi_m > 0$ and the other(s) have $\phi_m = 0$ [27, 37]. To better show this point, take for simplicity a binary polymer/vacancy mixture (Eq. (2), $\phi_s = 0$): here the critical point is for $\phi_m^* = 1/(1 + \sqrt{\ell})$ [2, 38], with the two branches of the binodal critical line lying to the left and to the right of it. As $\ell \rightarrow \infty$, both ϕ_m^* and the binodal left branch $\rightarrow 0$, therefore the value of ϕ_m for the polymer-poor phase must be also $= 0$ (Fig. 1 in [37]).

For a more complex ternary mixture of polymer, solvent and vacancies, we detail first the thermodynamics of separation in two phases, termed *I* and *II*, while three-phase coexistence is outlined in Sec. S2 in SM [18]. The generalization to multi-chain systems ($\ell < \infty$ at fixed ϕ_m) is discussed further below. Phase *I* is characterized by $\phi_m^I = 0$, $\phi_s^I > 0$ and occupies volume V^I , while phase *II* is characterized by $\phi_m^{II} > 0$, $\phi_s^{II} > 0$ and occupies volume V^{II} . By generalizing standard arguments for binary mixtures [38], these phases and their regions of stability

are determined by minimizing the total free energy

$$V^I f(0, \phi_s^I) + V^{II} f(\phi_m^{II}, \phi_s^{II}), \quad (3)$$

of the phase-separate system [39], with additional constraints on volume and particle number of each species:

$$V^I + V^{II} = V, \quad (4)$$

$$V^{II} \phi_m^{II} = V \phi_m, \quad (5)$$

$$V^I \phi_s^I + V^{II} \phi_s^{II} = V \phi_s, \quad (6)$$

where V is the total volume of the system and ϕ_m and ϕ_s are the densities at which the system is prepared. Minimization of Eq. (3) with constraints (4)-(6) *via* standard Lagrange multipliers leads to 5 coupled equations with 3 constraints that, by some manipulations, give:

$$\phi_s^I \left. \frac{\partial f}{\partial \phi_s} \right|_{\substack{\phi_m=0 \\ \phi_s=\phi_s^I}} - f(0, \phi_s^I) = \phi_m^{II} \left. \frac{\partial f}{\partial \phi_m} \right|_{\substack{\phi_m=\phi_m^{II} \\ \phi_s=\phi_s^{II}}} + \phi_s^{II} \left. \frac{\partial f}{\partial \phi_s} \right|_{\substack{\phi_m=\phi_m^{II} \\ \phi_s=\phi_s^{II}}} - f(\phi_m^{II}, \phi_s^{II}), \quad (7)$$

$$\left. \frac{\partial f}{\partial \phi_s} \right|_{\substack{\phi_m=0 \\ \phi_s=\phi_s^I}} = \left. \frac{\partial f}{\partial \phi_s} \right|_{\substack{\phi_m=\phi_m^{II} \\ \phi_s=\phi_s^{II}}}, \quad (8)$$

$$\phi_s^I = \frac{\phi_s \phi_m^{II} - \phi_m \phi_s^{II}}{\phi_m^{II} - \phi_m}. \quad (9)$$

Eqs. (7) and (8) can be easily identified as the balance of the osmotic pressures and the chemical potentials of the solvent in the two phases, while Eq. (9) is a generalization of the familiar lever rule for binary mixtures [2]. If, for a given pair (ϕ_m, ϕ_s) , a solution to Eqs. (7)-(9) exists, the system minimizes its free energy by phase separating into two coexisting phases and is in a *biphasic* region (see Sec. S2 in SM [18], for the discussion on the *triphasic* case); in polymer language, the chain collapses to a globule. The solution to Eqs. (7)-(9) is then used (Eqs. (4)-(6)) to infer V^I and V^{II} , so characterizing the two phases completely.

Convex hull construction and Gibbs triangle – Solution to Eqs. (7)-(9) (and analogues in Sec. S2 and Sec. S3 in SM [18]) requires a non-trivial numerical procedure [35, 36, 40]. The task, however, can be greatly simplified by looking at the “geometrical” meaning [41, 42] of these equations, *i.e.* the evaluation of the *lower convex hull* (l.c.h.) [43, 44] enveloping the free energy surface in the (ϕ_m, ϕ_s) -space. In particular, the regions where the shape of the l.c.h. differs from that of the free energy surface are those where phase separation occurs (in a binary mixture, this corresponds to the usual common tangent Maxwell construction, see Fig. 1 in [42]). In order to identify those regions (in particular, to distinguish biphasic from triphasic ones) we follow [41, 42] and reconstruct the shape of the l.c.h. by the accurate triangulation procedure introduced therein. We implement this method *via* the publicly available *Quickhull* package [44], and get an estimated phase diagram of the system that is then used in concert with the numerical solutions of Eqs. (7)-(9) and analogues in Sec. S2 and Sec. S3 in SM [18]. The obtained stable-phase solutions are represented in terms of the characteristic, and rather intuitive, *barycentric co-*

ordinates [35, 36, 45] of the Gibbs triangle (Fig. 2, (a) for a general description and (b) for a few tutorial examples).

Single-chain systems: results – We start by applying our theory to single-chain systems, and we focus on the particular problem [16] discussed in the Introduction: a single polymer represented by the Kremer-Grest bead-spring model [46] in explicit solvent conditions, where *mm* and *ss* interactions are described by the same attractive Lennard-Jones interaction. As the strength of the *ms* attraction (also of the Lennard-Jones type) increases, the chain swells as expected in standard good solvent conditions. However, by increasing the *ms* attraction even further, the polymer is observed to fold back thus giving a re-entrant collapse (Fig. S1(a) in SM [18]). To reproduce and rationalize this polymer behavior, consider the particular form of Eq. (2) with $\ell \rightarrow \infty$, $\epsilon_{mm} = \epsilon_{ss} = -\epsilon < 0$ and with $\epsilon_{ms} = -\lambda\epsilon < 0$ where $\lambda > 0$ tunes the *ms* attraction. By introducing $T^* \equiv k_B T / \epsilon$, we focus on phase stability of βf (2) as a function of densities ϕ_m and ϕ_s , parameters λ and T^* and, hereafter, in spatial dimensions $d = 3$. When the chosen densities (defining the mean composition of the system) do not belong to the stable region (as identified by the convex hull procedure), we solve numerically Eqs. (7)-(9) and (S32)-(S35) in SM [18] to determine the stable phases and represent the corresponding phase separation by a solid black line (a.k.a. a *tie-line*) in the Gibbs triangle.

To fix the ideas, we focus on the stability of 9 representative coordinates (ϕ_m, ϕ_s, ϕ_v) in the Gibbs triangle with the same $\phi_m = 0.1$, $\phi_s \in [0.05-0.85]$ and ϕ_v fixed accordingly (large blue dots in Fig. 3). First, we start by fixing the temperature $T^* = 2.5$ and increase λ systematically (Fig. 3): this corresponds to changing the solvent quality from “poor” to “good”. For $\lambda = 0.6$ (panel (a)), none of

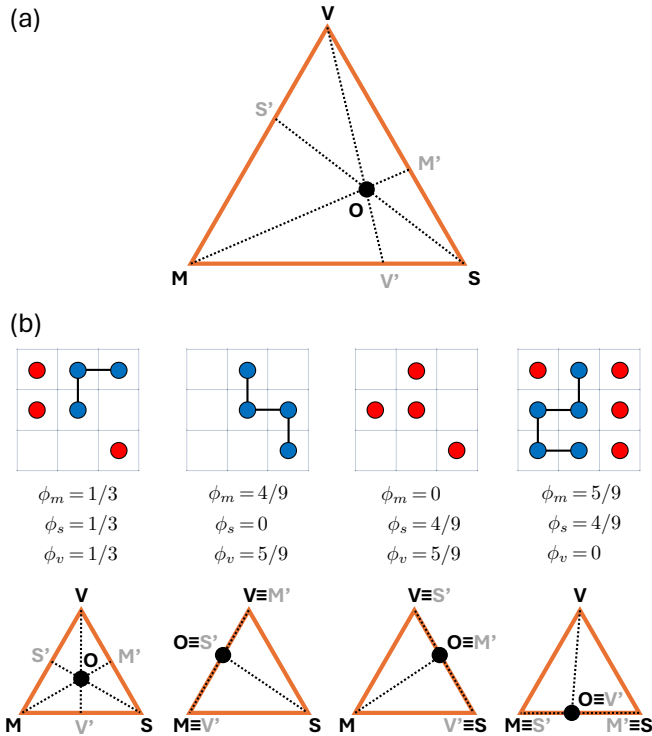


FIG. 2. (a) Gibbs triangle for a ternary mixture of monomers (vertex M), solvent molecules (vertex S) and vacancies (vertex V). A generic point O inside the triangle represents the state with densities $\phi_m = |OM'|/|MM'|$, $\phi_s = |OS'|/|SS'|$ and $\phi_v = |OV'|/|VV'|$, where “ $|\cdot|$ ” denotes the length of the segment. By elementary geometry, it is easily seen that $\phi_m + \phi_s + \phi_v = 1$. (b) Illustrative cases (dots’ color code is as in Fig. 1) on the 3×3 lattice, featuring: equipopulation of the three species (O is the triangle’s barycenter) and when one species is absent (O lies on the side opposite to the vertex).

the points is stable as they all lay in the biphasic region (light shaded area). This means that at this monomer concentration and temperature the system always phase separates in two different phases represented by the end small dots of each black line. One of these phases (lying on the SV edge) contains only solvent molecules and vacancies, mixed (see also Sec. S4 in SM [18]). The other phase (lying on the edge of the dark shaded region) is a polymer globule mixed with solvent molecules and vacancies [47]. As λ increases, the dark shaded region first touches the SV edge, and two of the original state points become stable (panel (b) for $\lambda = 0.76$) with the chain in the coil conformation as described earlier [37]. Upon further increase of λ more and more points are incorporated in the stable region up to $\lambda = 1.0$ (panel (c)); notice that, quite surprisingly, for low ϕ_s (or large ϕ_v), the system still phase-separates. Increasing λ further (panel (d)), a new feature emerges: the extension of the stable region decreases and some of the former stable points switch back to phase separation. This indeed represents the re-entrant globule phase described in [16] (Fig. S1(a) in SM [18]). Intriguingly, this re-entrance can be observed

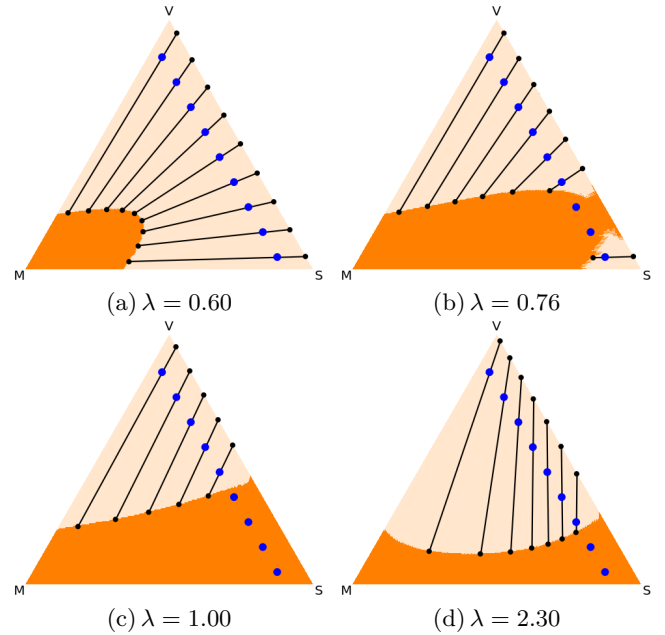


FIG. 3. Phase diagrams for single chain systems upon varying λ (Eq. (2) with $d = 3$, $\epsilon_{mm} = \epsilon_{ss} = -\epsilon < 0$, $\epsilon_{ms} = -\lambda\epsilon$ ($\lambda > 0$) and $T^* = k_B T / \epsilon = 2.5$). The dark- and light-shaded areas correspond, respectively, to the stable (coil) and the biphasic (globule) region as identified from the convex hull procedure (see text for details). Large blue dots correspond to 9 chosen mean compositions of the system with the same $\phi_m = 0.1$, while tiny black dots (connected by black lines) denote the compositions of the two stable phases in which the system separates. The positions of the black dots are calculated by solving numerically Eqs. (7)-(9).

only for “intermediate” ϕ_s : at high solvent densities the system remains in a coil state (at least, up to the value $\lambda = 2.3$ considered here), while at low ϕ_s the polymer never experiences the coil-globule transition and the system remains in the biphasic region at all λ ’s; the only significant modification is the compactness of the globule with the latter becoming more and more swollen as λ increases. Once more, this matches the findings of computer simulations by Garg *et al.* [17], that were performed at a much lower solvent density than Ref. [16]. There, however, the authors claimed a direct “transition” from a compact globule to a less compact one inflated by solvent molecules (Fig. S1(b) in SM [18]). Our result, instead, makes clear that the expansion is not a true thermodynamic transition but rather the result of the *continuous* modification of the coexistence line upon varying λ , with the system always remaining in a biphasic region.

Polymer collapse can be also achieved by fixing the ms interaction while decreasing the temperature. Here, this translates in fixing λ (we choose $\lambda = 0.7$) and in decreasing T^* (Fig. 4). At high T^* (panel (a)), the system separates in two phases only for very low ϕ_s . Then, as temperature drops (panels (b) and (c)), more and more

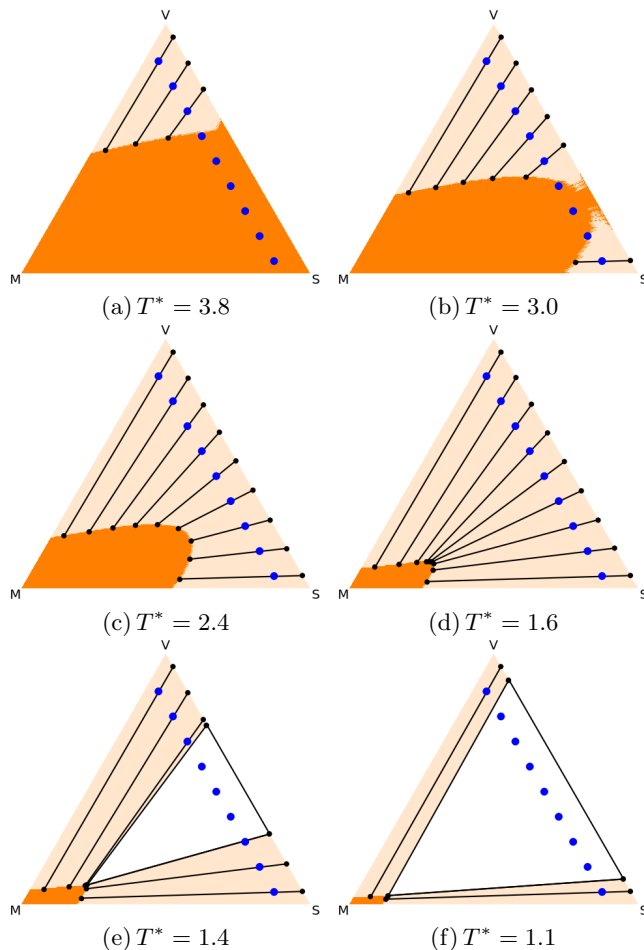


FIG. 4. Phase diagrams for single-chain system upon varying temperature (Eq. (2) with $d = 3$, $\epsilon_{mm} = \epsilon_{ss} = -\epsilon < 0$, $\epsilon_{ms} = -0.7\epsilon$ and selected values of $T^* = k_B T/\epsilon$). Symbols, color code and notation are as in Fig. 3. At high temperatures (panels (a) to (d)), system’s behavior is as seen in the two-phase situation. For $T^* < 1.5$ (panels (e) and (f)), triphasic stability (white triangular region, identified by the convex hull procedure) becomes possible: if the system is prepared inside this region, it separates into 3 coexisting phases whose compositions (obtained by solving numerically Eqs. (S32)-(S35) in SM [18]) lie at the corners of the white region.

points are incorporated in the two-phase region until, for $T^* < 1.5$ (Sec. S4 in SM [18]), a triphasic domain appears and extends progressively. The latter corresponds to the white triangle in panels (e) and (f), whose corners identifies the stable compositions into which the system separates; notice that two of these corners belong to the SV edge where $\phi_m = 0$. Contrary to previous cases, three-phase coexistence was *not* studied in past numerical simulations [16, 17] and our analysis indicates that it ought to be seen at sufficiently low temperatures.

As a further relevant application to single-chain systems, we revisit the recent “polymer-assisted condensation” [22] at the basis of the formation of biomolecular

condensates within cell nuclei: a two-component liquid mixture originally in a single stable phase is induced to phase-separate by the presence of a single polymer chain displaying preferential attachment to one of the two components. In our formalism, this condition can be easily reproduced by considering the solvent molecules and the vacancies as the original two-component mixture, with only ms and ss attractions ($\epsilon_{ss} = -\epsilon < 0$ and $\epsilon_{ms} < 0$) and purely steric mm interactions ($\epsilon_{mm} = 0$). Again, we take ϵ as the energy scale, with $T^* = k_B T/\epsilon$ and vary $\epsilon_{ms} = -\lambda\epsilon$ *via* λ . By setting $T^* = 1.3$ ($<$ the critical value = 1.5 for phase separation in the solvent-vacancy binary system, Secs. S1 C and S4 in SM [18]), we select 3 representative coordinates (ϕ_m, ϕ_s, ϕ_v) with solvent densities outside the *miscibility gap* [2] of the binary solvent-vacancy set-up and study their stability by varying λ . Remarkably (Fig. S2 in SM [18]), our theory reproduces the simulation results of Ref. [22]: for low λ (panel (a)) all three points are stable, while as λ increases (panels (b)-(d)) the early stable compositions phase-separate, beginning with those with the highest ϕ_s .

Multi-chain systems: results – The picture described so far can be extended to systems of multiple chains with a finite mean contour length ($\ell < \infty$). Here one has to solve a larger number of equations (Sec. S3 A and Sec. S3 B in SM [18]) to determine the coexistence lines, but otherwise there are no significant complications with respect to the single-chain case. Also for a multi-chain system, our MF theory predicts re-entrant phase behavior for increasing λ (Fig. S3 in SM [18]) that, interestingly, differs from the single-chain case since the polymer-poor phase is now characterized by a small, yet non-zero, value of the monomer density. In general, this is also in agreement with numerical simulations of polymer solutions (see Figs. 6 and 7 in [16]). Regrettably, the present approach does not allow to identify the spatial pattern of the condensed phase in this case, but in principle this could be achieved by introducing (see note [39]) proper surface tension terms between the different phases [42]. Finally, as in the single-chain case, the temperature dependence is also of particular interest and was not analyzed numerically before. Our theory predicts again that upon cooling there is a large region of the parameter space guaranteeing triphasic stability (white regions in Fig. S4 in SM [18]), especially panel (e) where we do recognize a polymer-poor phase with $\phi_m > 0$ that is absent in the single-chain case (compare to Fig. 4).

Conclusion – In this Letter, we have introduced a new $O(n \rightarrow 0)$ -vector spin model equivalent to the *exact* grand canonical partition function of lattice polymers with explicit solvent molecules (Eq. (1)), and mapped it to a field-theoretic form that is amenable to a saddle-point approximation. The resulting expression, via Legendre transform, gives the mean-field free energy of the system (βf , Eq. (2)) that generalizes earlier work [30, 31] and, notably, is of the Flory-Huggins form [20, 21] for a *ternary* mixture of polymer, solvent and vacancies. A systematic stability analysis of the equilibrium relations

for two (Eqs. (7)-(9) and Eqs. (S36)-(S39) in SM [18]) and three phases (Eqs. (S32)-(S35) and Eqs. (S40)-(S45) in SM [18]) by using the convex hull method [41, 42] of the free energy profile reproduces transparently recent results from extensive numerical simulations for single- and multi-chain systems in explicit solvent [16, 17, 22]. In particular, we provide a *unified* explanation for two seemingly unrelated observations: a re-entrant polymer coil-globule transition (Fig. 3) and polymer-assisted condensation of the solvent (Fig. S2 in SM [18]). Notice that although both transitions are triggered by increasing the strength of the attractive ms interaction, the role of vacancies (and the consequent entropy of the solvent) remains in both situations *essential*: these two phenomena are in fact absent altogether in a pure polymer/solvent binary mixture. Our approach enables us also to characterize in a transparent way the roles of *both*, solvent

density and temperature, that would otherwise require time-consuming computer simulations. In particular, we have discovered whole new regions of low-temperature three-phase stability (Fig. 4 and Fig. S4 in SM [18]) that were never described before. Finally, we point out that the main ideas and tools introduced here can be generalized to mixtures with more species, polymers with intrinsic bending stiffness [31] or polymers with complex architectures [48]. Work in that regard is currently under way.

Acknowledgements – A.G. acknowledges the MIUR PRIN-COFIN2022 grant 2022JWAF7YMIUR. A.G. and A.R. acknowledge networking support by the COST Action CA17139 (EUTOPIA). D.M. and A.R. acknowledge H. Schiessel for fruitful discussions, in particular for bringing to our attention the recent work on polymer-assisted condensation.

-
- [1] A. R. Khokhlov and A. Y. Grosberg, *Statistical Physics of Macromolecules* (AIP, New York, 1994).
- [2] M. Rubinstein and R. H. Colby, *Polymer Physics* (Oxford University Press, Oxford, 2003).
- [3] M. Doi, *Soft Matter Physics* (Oxford University Press, Oxford, 2013).
- [4] W. H. Stockmayer, *Makromol. Chem.* **35**, 54 (1960).
- [5] I. Lifshitz, A. Y. Grosberg, and A. Khokhlov, *J. Exp. Theor. Phys.* **44**, 855 (1976).
- [6] I. M. Lifshitz, A. Y. Grosberg, and A. R. Khokhlov, *Rev. Mod. Phys.* **50**, 683 (1978).
- [7] I. Nishio, S.-T. Sun, G. Swislow, and T. Tanaka, *Nature* **281**, 208 (1979).
- [8] G. Swislow, S.-T. Sun, I. Nishio, and T. Tanaka, *Phys. Rev. Lett.* **44**, 796 (1980).
- [9] G. Jannink and J. des Cloizeaux, *J. Phys. Condens. Matter* **2**, 1 (1990).
- [10] P. D. Olmsted, W. C. K. Poon, T. C. B. McLeish, N. J. Terrill, and A. J. Ryan, *Physical Review Letters* **81**, 373 (1998).
- [11] T. Arcangeli, T. Škrbić, S. Azote, D. Marcato, A. Rosa, J. R. Banavar, R. Piazza, A. Maritan, and A. Giacometti, “Phase behaviour and self-assembly of semiflexible polymers in poor-solvent solutions,” (2024), arXiv:2405.11287 [cond-mat.soft].
- [12] J. M. Polson and N. E. Moore, *J. Chem. Phys.* **122**, 024905 (2004).
- [13] J. M. Polson, S. B. Opps, and N. Abou Risk, *J. Chem. Phys.* **130**, 244902 (2009).
- [14] J. Heyda, A. Muzdalo, and J. Dzubiella, *Macromolecules* **46**, 1231 (2013).
- [15] Y. Zhao, M. K. Singh, K. Kremer, R. Cortes-Huerto, and D. Mukherji, *Macromolecules* **53**, 2101 (2020).
- [16] Y. Huang and S. Cheng, *J. Polym. Sci.* **59**, 2819 (2021).
- [17] H. Garg, R. Rajesh, and S. Vemparala, *J. Chem. Phys.* **158**, 114903 (2023).
- [18] See Supplemental Material at <http://XXX> for details of the analytical derivation of the grand canonical partition function and the mean-field approximation as well as some additional figures supporting main text.
- [19] R. Fantoni, A. Giacometti, and A. Santos, *J. Chem. Phys.* **142** (2015).
- [20] P. J. Flory, *J. Chem. Phys.* **10**, 51 (1942).
- [21] M. L. Huggins, *J. Phys. Chem.* **46**, 151 (1942).
- [22] J.-U. Sommer, H. Merlitz, and H. Schiessel, *Macromolecules* **55**, 4841 (2022).
- [23] A. A. Hyman, C. A. Weber, and F. Jülicher, *Annu. Rev. Cell Dev. Biol.* **30**, 39 (2014).
- [24] J. Berry, C. P. Brangwynne, and M. Haataja, *Rep. Prog. Phys.* **81**, 046601 (2018).
- [25] R. V. Pappu, S. R. Cohen, F. Dar, M. Farag, and M. Kar, *Chem. Rev.* **123**, 8945 (2023).
- [26] P. G. de Gennes, *Phys. Lett. A* **38**, 339 (1972).
- [27] P. G. de Gennes, *Scaling Concepts in Polymer Physics* (Cornell University Press, 1979).
- [28] H. Orland, C. Itzykson, and C. de Dominicis, *J. Physique Lett.* **46**, 353 (1985).
- [29] J. Bascle, T. Garel, and H. Orland, *J. Phys. A Math. Gen.* **25**, L1323 (1992).
- [30] S. Doniach, T. Garel, and H. Orland, *J. Chem. Phys.* **105**, 1601 (1996).
- [31] D. Marcato, A. Giacometti, A. Maritan, and A. Rosa, *J. Chem. Phys.* **159**, 154901 (2023).
- [32] As already observed in [31], a limitation of the grand canonical approach is that it is not able to predict the presence of an ordered (crystalline) phase: the disordered phase is entropically favored because of polydispersity.
- [33] It reduces, in particular, to the expression derived by us in [31] (see Eq. (61) therein) for the simplest situation where the solvent is absent (*i.e.*, for $\phi_s = 0$).
- [34] M. G. Bawendi and K. F. Freed, *J. Chem. Phys.* **88**, 2741 (1988).
- [35] H. Tompa, *Trans. Faraday Soc.* **45**, 1142 (1949).
- [36] F. W. Altena and C. Smolders, *Macromolecules* **15**, 1491 (1982).
- [37] W. Paul, T. Strauch, F. Rampf, and K. Binder, *Phys. Rev. E* **75**, 060801 (2007).
- [38] D. Qian, T. C. Michaels, and T. P. Knowles, *J. Phys. Chem. Lett.* **13**, 7853 (2022).
- [39] Eq. (3) neglects explicitly surface tension contributions between different phases. This approximation is recurrent

in our theory.

- [40] The numerical solution to Eqs. (7)-(9) (and analogues in Sec. S2 and Sec. S3 in SM [18]) has been programmed in-house by using Mathematica. The codes are freely available at: <https://github.com/davideMarcato/coexistence.equations>.
- [41] J. Wolff, C. M. Marques, and F. Thalmann, Phys. Rev. Lett. **106**, 128104 (2011).
- [42] S. Mao, D. Kuldinow, H. P. Mikko, and A. Košmrlj, Soft Matter **15**, 1297 (2019).
- [43] F. P. Preparata and M. I. Shamos, Computational Geometry: An Introduction (Springer Science & Business Media, 2012).
- [44] C. B. Barber, D. P. Dobkin, and H. Huhdanpaa, ACM Trans. Math. Softw. **22**, 469–483 (1996).
- [45] R. J. Howarth, The British Journal for the History of Science **29**, 337–356 (1996).
- [46] K. Kremer and G. S. Grest, The Journal of Chemical Physics **92**, 5057 (1990).
- [47] It is worthwhile recalling that solvent molecules and vacancies are *not* interchangeable as monomers interact with solvent molecules but not with vacancies.
- [48] T. C. Lubensky and J. Isaacson, Phys. Rev. A **20**, 2130 (1979).
- [49] Our formalism applies to polymer contour lengths beyond the so called Kuhn length [2] of the chain. As noticed in [31], introducing bending stiffness implies only a “redefinition” of chain and bond fugacities κ_c and κ_b , that would not affect the conclusions here.
- [50] J. Hubbard, Phys. Rev. Lett. **3**, 77 (1959).
- [51] P. M. Chaikin and T. C. Lubensky, Principles of Condensed Matter Physics (Cambridge University Press, 2000).
- [52] Specifically, by this ansatz every dependence on n disappears, therefore the limit $n \rightarrow 0$ becomes trivial.
- [53] For the parsimony of notation, we adopt the same symbols “ φ ” and “ ψ_σ ” also for the *solutions* of MF equations (S15)-(S18).

Supplemental Material

Assessing Polymer Phase Behavior in Explicit Solvent and with Vacancies

Davide Marcato, Achille Giacometti, Amos Maritan, Angelo Rosa

CONTENTS

References	6
S1. Microscopic lattice model	S2
A. Definition	S2
B. Mean-field (saddle-point) formulation	S3
C. Free energy of the system	S4
S2. Single-chain systems: three-phase stability	S4
S3. Multi-chain systems	S5
A. Two-phase stability	S5
B. Three-phase stability	S6
S4. Binary mixtures as special cases	S6
Supplemental figures	S7

S1. MICROSCOPIC LATTICE MODEL

A. Definition

The model adapts and generalizes the language of our field-theoretical formalism [31] for self-interacting polymers on the d -dimensional hypercubic lattice by taking into account the explicit role of solvent molecules. We take the elementary lattice step as our unit of length and we denote by N the total number of sites of the (hypercubic) lattice. For simplicity, monomers and solvent molecules have the same “size”, namely one monomer or one solvent molecule occupy one single lattice site; at the same time, to enforce the natural constraint of excluded volume, each lattice site is either empty or occupied at most by one single molecular species (either a monomer or a solvent molecule) otherwise double-occupancy is strictly forbidden. Importantly, the whole lattice may be not completely filled (*i.e.*, lattice vacancies are present) and we consider the situation of completely flexible chains, namely the bond length of the chains is equal to one lattice unit (see footnote [49]).

As explained in detail in the main text, our starting point is the grand canonical partition function $Z = Z(\kappa_c, \kappa_b, \kappa_s, \epsilon_{mm}, \epsilon_{ss}, \epsilon_{ms})$ (see Eq. (1) in the main text and the related definitions for the different quantities). By introducing [31] at each lattice position \mathbf{x} the n -component vector $\mathbf{S}(\mathbf{x}) \equiv (S^1(\mathbf{x}), S^2(\mathbf{x}), \dots, S^n(\mathbf{x}))$ with the *internal product* $\mathbf{S}(\mathbf{x}) \cdot \mathbf{S}(\mathbf{x}') \equiv \sum_{i=1}^n S^i(\mathbf{x}) S^i(\mathbf{x}')$ between any two vectors associated to lattice points \mathbf{x} and \mathbf{x}' and by defining the *trace* operation (denoted by the symbol $\langle \dots \rangle_0$) through the formal rules:

$$\langle 1 \rangle_0 = 1, \quad (S1)$$

$$\langle S^i \rangle_0 = 0, \quad (S2)$$

$$\langle S^i S^j \rangle_0 = \delta_{ij}, \quad (S3)$$

$$\langle S^{i_1} S^{i_2} \dots S^{i_k} \rangle_0 = 0, \text{ if } k \geq 3, \quad (S4)$$

with S -vectors on different sites being independent from each other under the same trace operation, the following identity holds (compare to Eq. (32) in [31])

$$Z = \int \prod_{\sigma} \mathcal{D}\psi_{\sigma} \exp\left(-\frac{1}{2} \sum_{\sigma} \sum_{\vec{x}, \vec{x}'} \Delta^{-1}(\mathbf{x}, \mathbf{x}') \psi_{\sigma}(\mathbf{x}) \psi_{\sigma}(\mathbf{x}')\right) \times \lim_{n \rightarrow 0} \left\langle \prod_{\mathbf{x}} \left(1 + H_c(\mathbf{x}) S^1(\mathbf{x}) + H_s(\mathbf{x}) (S^1(\mathbf{x}))^2\right) \exp\left[\frac{1}{2} \sum_{\mathbf{x}, \mathbf{x}'} \Delta(\mathbf{x}, \mathbf{x}') h(\mathbf{x}) h(\mathbf{x}') \mathbf{S}(\mathbf{x}) \cdot \mathbf{S}(\mathbf{x}')\right]\right\rangle_0, \quad (S5)$$

where:

$$\Delta(\mathbf{x}, \mathbf{x}') = \begin{cases} 1, & \text{if } |\mathbf{x} - \mathbf{x}'| = 1 \text{ lattice step} \\ 0, & \text{otherwise} \end{cases}, \quad (S6)$$

$$H_c(\mathbf{x}) = \sqrt{\kappa_c} e^{\frac{\sqrt{\beta(\epsilon_{ms} - \epsilon_{mm})}}{2} \psi_{mm}(\mathbf{x}) + \frac{\sqrt{-\beta\epsilon_{ms}}}{2} \psi_{ms}(\mathbf{x})}, \quad (S7)$$

$$H_s(\mathbf{x}) = \kappa_s e^{\sqrt{\beta(\epsilon_{ms} - \epsilon_{mm})} \psi_{ss}(\mathbf{x}) + \sqrt{-\beta\epsilon_{ms}} \psi_{ms}(\mathbf{x})}, \quad (S8)$$

$$h(\mathbf{x}) = \sqrt{\kappa_b} e^{\frac{\beta\epsilon_{mm}}{2}} e^{\frac{\sqrt{\beta(\epsilon_{ms} - \epsilon_{mm})}}{2} \psi_{mm}(\mathbf{x}) + \frac{\sqrt{-\beta\epsilon_{ms}}}{2} \psi_{ms}(\mathbf{x})}, \quad (S9)$$

$\mathcal{D}\psi_{\sigma} \equiv (2\pi)^{-N/2} (\det \Delta)^{-1/2} \prod_{\vec{x}} d\psi_{\sigma}(\mathbf{x})$ is the measure associated to the auxiliary scalar fields $\psi_{\sigma} = \psi_{\sigma}(\mathbf{x})$ with $\sigma = \{mm, ms, ss\}$ (*i.e.*, there are 3 scalar fields per each lattice site) and – importantly! – the “ $\lim_{n \rightarrow 0}$ ” operation is required [31] to rule out all contributions to the partition function that include chain topologies different from the linear one. Then, the last step consists in “removing” the dependence on the \mathbf{S} -vectors in the last term of Eq. (S5) in favor of the vector field $\boldsymbol{\varphi}(\mathbf{x}) \equiv (\varphi^1(\mathbf{x}), \varphi^2(\mathbf{x}), \dots, \varphi^n(\mathbf{x}))$ with the associated measure

$$\mathcal{D}\boldsymbol{\varphi} \equiv (2\pi)^{-nN/2} (\det \Delta)^{-n/2} \prod_{\mathbf{x}} d\boldsymbol{\varphi}(\mathbf{x}), \quad (S10)$$

by means of a standard Hubbard-Stratonovich transformation [50, 51]. After some manipulations, and up to an unimportant prefactor, the grand canonical partition function takes the final form:

$$Z = \lim_{n \rightarrow 0} \int \prod_{\mathbf{x}} \prod_{\sigma} d\psi_{\sigma}(\mathbf{x}) \int \prod_{\mathbf{x}} d\boldsymbol{\varphi}(\mathbf{x}) \exp\left\{-A - B + \sum_{\mathbf{x}} \ln[1 + C]\right\}, \quad (S11)$$

where:

$$A = \frac{1}{2} \sum_{\sigma} \sum_{\mathbf{x}, \mathbf{x}'} \Delta^{-1}(\mathbf{x}, \mathbf{x}') \psi_{\sigma}(\mathbf{x}) \psi_{\sigma}(\mathbf{x}'), \quad (\text{S12})$$

$$B = \frac{1}{2} \sum_{\mathbf{x}, \mathbf{x}'} \Delta^{-1}(\mathbf{x}, \mathbf{x}') \boldsymbol{\varphi}(\mathbf{x}) \cdot \boldsymbol{\varphi}(\mathbf{x}'), \quad (\text{S13})$$

$$C = H_s(\mathbf{x}) + \frac{h^2(\mathbf{x})}{2} |\boldsymbol{\varphi}(\mathbf{x})|^2 + H_c(\mathbf{x}) h(\mathbf{x}) \varphi^1(\mathbf{x}). \quad (\text{S14})$$

B. Mean-field (saddle-point) formulation

Despite being formally exact, Eq. (S11) can not be evaluated directly. This field-theoretic form is however particularly suitable for an expansion around the saddle-point [28–31]. In order to compute the first term of such expansion, we differentiate the exponential in Eq. (S11) with respect to each $\varphi^i(\mathbf{x})$ and $\psi_{\sigma}(\mathbf{x})$ and set the obtained expressions equal to 0. Then, we simplify the problem further by looking only for those solutions that both (i) satisfy translational invariance and (ii) break the $O(n)$ symmetry of the vector field [52], *i.e.* $\boldsymbol{\varphi}(\mathbf{x}) = (\varphi, 0, \dots, 0)$ and $\psi_{\sigma}(\mathbf{x}) = \psi_{\sigma}$ for every \mathbf{x} , that leads to:

$$\frac{\varphi}{2d} = \frac{h^2 \varphi + H_c h}{1 + H_s + \frac{h^2}{2} \varphi^2 + H_c h \varphi}, \quad (\text{S15})$$

$$\frac{\psi_{mm}}{2d} = \frac{\sqrt{\beta(\epsilon_{ms} - \epsilon_{mm})} \left(\frac{h^2}{2} \varphi^2 + H_c h \varphi \right)}{1 + H_s + \frac{h^2}{2} \varphi^2 + H_c h \varphi}, \quad (\text{S16})$$

$$\frac{\psi_{ss}}{2d} = \frac{\sqrt{\beta(\epsilon_{ms} - \epsilon_{ss})} H_s}{1 + H_s + \frac{h^2}{2} \varphi^2 + H_c h \varphi}, \quad (\text{S17})$$

$$\frac{\psi_{ms}}{2d} = \frac{\sqrt{-\beta \epsilon_{ms}} \left(H_s + \frac{h^2}{2} \varphi^2 + H_c h \varphi \right)}{1 + H_s + \frac{h^2}{2} \varphi^2 + H_c h \varphi}, \quad (\text{S18})$$

where H_c , H_s and h are the same quantities defined in Eqs. (S7)-(S9), computed in correspondence of the saddle-point. In terms of the solutions [53] $\boldsymbol{\varphi} = \boldsymbol{\varphi}(\kappa_c, \kappa_b, \kappa_s, \epsilon_{mm}, \epsilon_{ss}, \epsilon_{ms})$ and $\psi_{\sigma} = \psi_{\sigma}(\kappa_c, \kappa_b, \kappa_s, \epsilon_{mm}, \epsilon_{ss}, \epsilon_{ms})$ of the MF Eqs. (S15)-(S18), the corresponding grand potential per lattice site, $\beta\Omega \equiv -\ln(Z)/N$, reads (up to an unimportant additive constant) as the following:

$$\beta\Omega(\kappa_c, \kappa_b, \kappa_s, \epsilon_{mm}, \epsilon_{ss}, \epsilon_{ms}) = \frac{\psi_{mm}^2}{4d} + \frac{\psi_{ms}^2}{4d} + \frac{\psi_{ss}^2}{4d} + \frac{\varphi^2}{4d} - \ln \left[1 + H_s + H_c h \varphi + \frac{h^2}{2} \varphi^2 \right]. \quad (\text{S19})$$

Eq. (S19), alongside Eqs. (S15)-(S18) and Eqs. (S7)-(S9) calculated at the saddle-point, defines completely the thermodynamics of the system. In particular, it is easy to derive the following expressions:

$$\phi_c \equiv \frac{\langle N_c \rangle}{N} = -\beta \kappa_c \frac{\partial \Omega}{\partial \kappa_c} = \frac{1}{2} \frac{H_c h \varphi}{1 + H_s + H_c h \varphi + \frac{h^2}{2} \varphi^2}, \quad (\text{S20})$$

$$\phi_b \equiv \frac{\langle N_b \rangle}{N} = -\beta \kappa_b \frac{\partial \Omega}{\partial \kappa_b} = \frac{\varphi^2}{4d}, \quad (\text{S21})$$

$$\phi_m \equiv \phi_c + \phi_b = \frac{\frac{h^2}{2} \varphi^2 + H_c h \varphi}{1 + H_s + H_c h \varphi + \frac{h^2}{2} \varphi^2}, \quad (\text{S22})$$

$$\phi_s \equiv \frac{\langle N_s \rangle}{N} = -\beta \kappa_s \frac{\partial \Omega}{\partial \kappa_s} = \frac{H_s}{1 + H_s + H_c h \varphi + \frac{h^2}{2} \varphi^2}, \quad (\text{S23})$$

for, respectively, the (mean) chain, bond, monomer and solvent fraction or density.

C. Free energy of the system

An alternative, more convenient way to characterize the thermodynamics of the system is by means of the free energy per lattice site,

$$\beta f = \beta f(\phi_c, \phi_b, \phi_s) \equiv \beta \Omega + \phi_c \ln \kappa_c + \phi_b \ln \kappa_b + \phi_s \ln \kappa_s, \quad (\text{S24})$$

which is the Legendre transform [31] of the grand potential $\beta \Omega$ (S19), and where the fugacities

$$\kappa_c = \frac{2\phi_c^2}{(\phi_b - \phi_c)(1 - \phi_m - \phi_s)} e^{2d\beta(\epsilon_{mm}\phi_m + \epsilon_{ms}\phi_s)}, \quad (\text{S25})$$

$$\kappa_b = \frac{\phi_b - \phi_c}{2d\phi_b(1 - \phi_m - \phi_s)} e^{2d\beta(\epsilon_{mm}\phi_m + \epsilon_{ms}\phi_s) - \beta\epsilon_{mm}}, \quad (\text{S26})$$

$$\kappa_s = \frac{\phi_s}{1 - \phi_m - \phi_s} e^{2d\beta(\epsilon_{mm}\phi_m + \epsilon_{ss}\phi_s)}, \quad (\text{S27})$$

are given (see Eqs. (S20)-(S23)) as a function of densities ϕ_m , ϕ_s and $\phi_c = \phi_m/\ell$ where ℓ is the *mean* length of the polymer chains (remember that within this model the system is intrinsically polydisperse, see main text). By straightforward calculations, one finally obtains the free energy expression, βf , reported in Eq. (2) in the main text.

It is instructive to specialize βf to *binary* mixtures, namely when one of the three considered species (monomers (m), solvent molecules (s) or vacancies (v)) is absent. In particular, by subtracting the contribution of the free energy for the phase-separated system, we get the functional form of the free energy of *mixing* and the related *Flory parameter*, χ , recapitulating the interaction between the two species (for reference, see [2, 27]). Three situations are possible:

1. $\phi_m = 0$: $\beta f = \beta f(\phi_s) = d\beta\epsilon_{ss}\phi_s^2 + (1 - \phi_s) \ln(1 - \phi_s) + \phi_s \ln(\phi_s)$ corresponds to the free energy of a mixture of solvent molecules and vacancies. By the corresponding free energy of *mixing* $-\beta\Delta f(\phi_s) \equiv \beta f(\phi_s) - \phi_s \beta f(\phi_s = 1)$ – the Flory parameter for the solvent molecules is $\chi = -d\beta\epsilon_{ss}$. Accordingly, aggregation of solvent particles happens at the *critical* Flory parameter $\chi_c = 2$, corresponding to the critical temperature $T_c = -\frac{d\epsilon_{ss}}{2k_B}$ (obviously, physical values of T_c are possible only for $\epsilon_{ss} < 0$, namely when solvent molecules attract each other).
2. $\phi_s = 0$: $\beta f = \beta f(\phi_m, \ell) = d\beta\epsilon_{mm}\phi_m^2 + (1 - \phi_m) \ln(1 - \phi_m) + \frac{\phi_m}{\ell} \ln(\phi_m) + \phi_m \ln\left(\frac{(1-2/\ell)^{1-2/\ell} (2/\ell^2)^{1/\ell}}{(2d e^{\beta\epsilon_{mm}-1} (1-1/\ell))^{1-1/\ell}}\right)$ corresponds to the free energy of a mixture of polymer chains of mean contour length ℓ and vacancies. Now the free energy of mixing $-\beta\Delta f(\phi_m) \equiv \beta f(\phi_m) - \phi_m \beta f(\phi_m = 1)$ – gives the Flory parameter for the polymer molecules $\chi = -d\beta\epsilon_{mm}$. The critical temperature of aggregation of polymer chains is particularly easy to calculate in the two limit cases: (i) for $\ell = 1$, this is analogous to the case of solvent particles and $T_c = -\frac{d\epsilon_{mm}}{2k_B}$; (ii) for $\ell \rightarrow \infty$, this reduces to the case by Doniach *et al.* [30] where $T_c = -\frac{2d\epsilon_{mm}}{k_B}$.
3. $\phi_v = 1 - \phi_m - \phi_s = 0$: $\beta f(\phi_m, \ell) = d\beta\epsilon_{mm}\phi_m^2 + d\beta\epsilon_{ss}(1 - \phi_m)^2 + 2d\beta\epsilon_{ms}\phi_m(1 - \phi_m) + \frac{\phi_m}{\ell} \ln(\phi_m) + (1 - \phi_m) \ln(1 - \phi_m) + \phi_m \ln\left(\frac{(1-2/\ell)^{1-2/\ell} (2/\ell^2)^{1/\ell}}{(2d e^{\beta\epsilon_{mm}-1} (1-1/\ell))^{1-1/\ell}}\right)$ corresponds to the free energy of a mixture of polymer chains of mean contour length ℓ and solvent molecules. By the same procedure as before, the free energy of mixing $-\beta\Delta f(\phi_m) \equiv \beta f(\phi_m) - \phi_m \beta f(\phi_m = 1) - (1 - \phi_m) \beta f(\phi_m = 0)$ – gives the Flory parameter for the polymer/solvent mixture $\chi = d\beta(2\epsilon_{ms} - \epsilon_{mm} - \epsilon_{ss})$. Now, the critical temperatures for phase separation in the two limit cases discussed at point (2) are: (i) for $\ell = 1$, $T_c = \frac{d(2\epsilon_{ms} - \epsilon_{mm} - \epsilon_{ss})}{2k_B}$; (ii) for $\ell \rightarrow \infty$, $T_c = \frac{2d(2\epsilon_{ms} - \epsilon_{mm} - \epsilon_{ss})}{k_B}$.

The special cases (1)-(3) will be viewed again in Sec. S4, in relation to the numerical solution to the complete free energy of the ternary mixture (Eq. (2) in the main text).

S2. SINGLE-CHAIN SYSTEMS: THREE-PHASE STABILITY

In order to derive the conditions for the coexistence of three phases in single-chain systems we proceed similarly as for the case of two phases. The starting point is the total free energy of the phase-separated system (compare to Eq. (3) in the main text),

$$V^I f(0, \phi_s^I) + V^{II} f(0, \phi_s^{II}) + V^{III} f(\phi_m^{III}, \phi_s^{III}), \quad (\text{S28})$$

with the constraints (compare to Eqs. (4)-(6) in the main text):

$$V^I + V^{II} + V^{III} = V, \quad (\text{S29})$$

$$V^{III} \phi_m^{III} = V \phi_m, \quad (\text{S30})$$

$$V^I \phi_s^I + V^{II} \phi_s^{II} + V^{III} \phi_s^{III} = V \phi_s. \quad (\text{S31})$$

This time, the minimization procedure leads to a system of 7 equations (with 3 constraints), that can be rearranged into the following relations for the equilibrium densities:

$$\phi_s^I \frac{\partial f}{\partial \phi_s} \Big|_{\substack{\phi_m=0 \\ \phi_s=\phi_s^I}} - f(0, \phi_s^I) = \phi_s^{II} \frac{\partial f}{\partial \phi_s} \Big|_{\substack{\phi_m=0 \\ \phi_s=\phi_s^{II}}} - f(0, \phi_s^{II}), \quad (\text{S32})$$

$$\phi_s^I \frac{\partial f}{\partial \phi_s} \Big|_{\substack{\phi_m=0 \\ \phi_s=\phi_s^I}} - f(0, \phi_s^I) = \phi_m^{III} \frac{\partial f}{\partial \phi_m} \Big|_{\substack{\phi_m=\phi_m^{III} \\ \phi_s=\phi_s^{III}}} + \phi_s^{III} \frac{\partial f}{\partial \phi_s} \Big|_{\substack{\phi_m=\phi_m^{III} \\ \phi_s=\phi_s^{III}}} - f(\phi_m^{III}, \phi_s^{III}), \quad (\text{S33})$$

$$\frac{\partial f}{\partial \phi_s} \Big|_{\substack{\phi_m=0 \\ \phi_s=\phi_s^I}} = \frac{\partial f}{\partial \phi_s} \Big|_{\substack{\phi_m=0 \\ \phi_s=\phi_s^{II}}}, \quad (\text{S34})$$

$$\frac{\partial f}{\partial \phi_s} \Big|_{\substack{\phi_m=0 \\ \phi_s=\phi_s^I}} = \frac{\partial f}{\partial \phi_s} \Big|_{\substack{\phi_m=\phi_m^{III} \\ \phi_s=\phi_s^{III}}}. \quad (\text{S35})$$

Again, if a non-trivial solution to Eqs. (S32)-(S35) exists, then the system minimizes its free energy by separating into three coexisting phases. An interesting difference with respect to the biphasic case (compare to Eqs. (7)-(9) in the main text) is that the solution to Eqs. (S32)-(S35) *does not* depend explicitly on the average densities ϕ_m and ϕ_s . Three-phase stability is illustrated in Fig. 4 in the main text.

S3. MULTI-CHAIN SYSTEMS

In this Section, we describe the conditions for two-phase (Sec. S3A) and three-phase (Sec. S3B) stability for a polymer solution in explicit solvent, assuming chains of *finite* mean contour length (*i.e.*, $\ell < \infty$ in Eq. (2) in the main text).

A. Two-phase stability

Contrarily to the single-chain case, in the derivation of the equations for the equilibrium densities (namely, the equivalent of Eqs. (7)-(9) in the main text), we can not assume that one of the phases in which the system separates has $\phi_m = 0$. Based on that, and by adopting the same notation of the main text, for the two-phase case we have to determine $\phi_m^I > 0$ in addition to all the other quantities. After some math, the new set of equations becomes:

$$\phi_m^I \frac{\partial f}{\partial \phi_m} \Big|_{\substack{\phi_m=\phi_m^I \\ \phi_s=\phi_s^I}} + \phi_s^I \frac{\partial f}{\partial \phi_s} \Big|_{\substack{\phi_m=\phi_m^I \\ \phi_s=\phi_s^I}} - f(\phi_m^I, \phi_s^I) = \phi_m^{II} \frac{\partial f}{\partial \phi_m} \Big|_{\substack{\phi_m=\phi_m^{II} \\ \phi_s=\phi_s^{II}}} + \phi_s^{II} \frac{\partial f}{\partial \phi_s} \Big|_{\substack{\phi_m=\phi_m^{II} \\ \phi_s=\phi_s^{II}}} - f(\phi_m^{II}, \phi_s^{II}), \quad (\text{S36})$$

$$\frac{\partial f}{\partial \phi_m} \Big|_{\substack{\phi_m=\phi_m^I \\ \phi_s=\phi_s^I}} = \frac{\partial f}{\partial \phi_m} \Big|_{\substack{\phi_m=\phi_m^{II} \\ \phi_s=\phi_s^{II}}}, \quad (\text{S37})$$

$$\frac{\partial f}{\partial \phi_s} \Big|_{\substack{\phi_m=\phi_m^I \\ \phi_s=\phi_s^I}} = \frac{\partial f}{\partial \phi_s} \Big|_{\substack{\phi_m=\phi_m^{II} \\ \phi_s=\phi_s^{II}}}, \quad (\text{S38})$$

$$\frac{\phi_m - \phi_m^I}{\phi_m^{II} - \phi_m^I} = \frac{\phi_s - \phi_s^I}{\phi_s^{II} - \phi_s^I}. \quad (\text{S39})$$

Notice in particular, and in comparison to Eqs. (7)-(9) in the main text, the “new” Eq. (S37) as the consequence of having $\phi_m^I > 0$. Moreover, and as already noticed for $\ell \rightarrow \infty$, also in this more general case the solution to Eqs. (S36)-(S39) depends explicitly on the preparation conditions of the system, ϕ_m and ϕ_s .

Two-phase stability for multi-chain systems is illustrated in Fig. S3 for the same set of parameters considered in Fig. 3 in the main text and chain mean length $\ell = 10$. The major difference with respect to the single-chain case

is in the appearance of a dilute, yet strictly non-zero, polymer phase that, intuitively, is expected to become more pronounced for lower values of ℓ . Finally, as can be noticed in Fig. S3, a re-entrance condition does still exist for $\lambda > 1.0$, in agreement with the results of molecular dynamics computer simulations by Huang and Cheng [16].

B. Three-phase stability

The last case to be addressed is that of three-phase coexistence in multi-chain system. Again, the main difference with respect to the single-chain counterpart is that we can no longer assume that $\phi_m = 0$ in any of the phases in which the system separates. Therefore, in total we need now to compute 6 equilibrium densities. By implementing the same procedure of the minimization of the free energy (Eq. (2) in the main text) with the proper constraints leads to the following equations:

$$\phi_m^I \frac{\partial f}{\partial \phi_m} \Big|_{\substack{\phi_m=\phi_m^I \\ \phi_s=\phi_s^I}} + \phi_s^I \frac{\partial f}{\partial \phi_s} \Big|_{\substack{\phi_m=\phi_m^I \\ \phi_s=\phi_s^I}} - f(\phi_m^I, \phi_s^I) = \phi_m^{II} \frac{\partial f}{\partial \phi_m} \Big|_{\substack{\phi_m=\phi_m^{II} \\ \phi_s=\phi_s^{II}}} + \phi_s^{II} \frac{\partial f}{\partial \phi_s} \Big|_{\substack{\phi_m=\phi_m^{II} \\ \phi_s=\phi_s^{II}}} - f(\phi_m^{II}, \phi_s^{II}), \quad (\text{S40})$$

$$\phi_m^I \frac{\partial f}{\partial \phi_m} \Big|_{\substack{\phi_m=\phi_m^I \\ \phi_s=\phi_s^I}} + \phi_s^I \frac{\partial f}{\partial \phi_s} \Big|_{\substack{\phi_m=\phi_m^I \\ \phi_s=\phi_s^I}} - f(\phi_m^I, \phi_s^I) = \phi_m^{III} \frac{\partial f}{\partial \phi_m} \Big|_{\substack{\phi_m=\phi_m^{III} \\ \phi_s=\phi_s^{III}}} + \phi_s^{III} \frac{\partial f}{\partial \phi_s} \Big|_{\substack{\phi_m=\phi_m^{III} \\ \phi_s=\phi_s^{III}}} - f(\phi_m^{III}, \phi_s^{III}), \quad (\text{S41})$$

$$\frac{\partial f}{\partial \phi_m} \Big|_{\substack{\phi_m=\phi_m^I \\ \phi_s=\phi_s^I}} = \frac{\partial f}{\partial \phi_m} \Big|_{\substack{\phi_m=\phi_m^{II} \\ \phi_s=\phi_s^{II}}}, \quad (\text{S42})$$

$$\frac{\partial f}{\partial \phi_m} \Big|_{\substack{\phi_m=\phi_m^I \\ \phi_s=\phi_s^I}} = \frac{\partial f}{\partial \phi_m} \Big|_{\substack{\phi_m=\phi_m^{III} \\ \phi_s=\phi_s^{III}}}, \quad (\text{S43})$$

$$\frac{\partial f}{\partial \phi_s} \Big|_{\substack{\phi_m=\phi_m^I \\ \phi_s=\phi_s^I}} = \frac{\partial f}{\partial \phi_s} \Big|_{\substack{\phi_m=\phi_m^{II} \\ \phi_s=\phi_s^{II}}}, \quad (\text{S44})$$

$$\frac{\partial f}{\partial \phi_s} \Big|_{\substack{\phi_m=\phi_m^I \\ \phi_s=\phi_s^I}} = \frac{\partial f}{\partial \phi_s} \Big|_{\substack{\phi_m=\phi_m^{III} \\ \phi_s=\phi_s^{III}}}. \quad (\text{S45})$$

Once again, we notice that Eqs. (S40)-(S45) imply the equality of the osmotic pressure and the chemical potential of both species (monomers and solvent molecules) in all 3 phases.

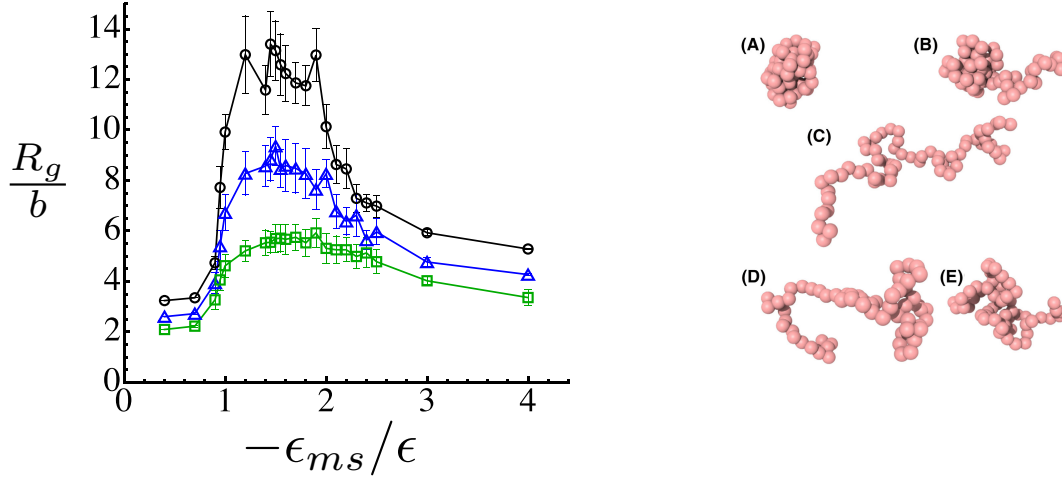
S4. BINARY MIXTURES AS SPECIAL CASES

The numerical results presented in Fig. 3 and Fig. 4 in the main text are in perfect agreement with the limit cases where one of the species is absent (see the related discussion in Sec. S1C):

1. $\phi_m = 0$: A binary mixture of solvent molecules and vacancies is represented as a point on the SV side of the Gibbs triangle. Here the critical temperature $T_c^* = d/2$ ($= 3/2$ for $d = 3$): accordingly, for $T^* < T_c^*$ some points on the SV sides become non-stable and a triphasic region appears (see Fig. 4).
2. $\phi_s = 0$: A system with no solvent molecules corresponds to a point on the side MV . Now the critical temperature $T_c^* = 2d$ ($= 6$ for $d = 3$): for $T^* < T_c^*$ the system phase-separates and the density of the globule is given by the binodal line, that depends only on temperature. Therefore, at fixed T^* , the stability of the MV side should not change: this is easily noticed in Fig. 3 in the main text.
3. $\phi_v = 1 - \phi_m - \phi_s = 0$: Finally, a system with no vacancies is represented by a point on the MS side. In these conditions, the critical temperature $T_c^* = 4d(1 - \lambda)$ ($= 12(1 - \lambda)$ for $d = 3$). Therefore, for $\lambda > 1$ the entire MS side is expected to be in the stable region, regardless of the value of T^* . For the example shown in Fig. 4, $\lambda = 0.7$ and $T_c^* = 3.6$ for the MS system: indeed, at $T^* = 3.8$ (panel (f)) the entire MS side is contained in the stable region.

SUPPLEMENTAL FIGURES

(a) Huang & Cheng, J Pol Sci (2021)



(b) Garg et al., J Chem Phys (2023)

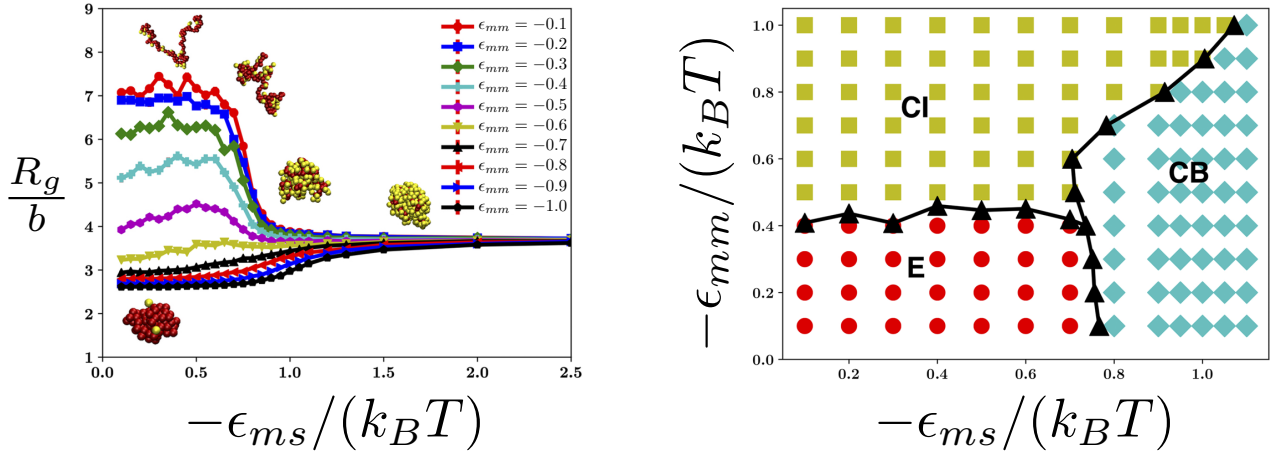


FIG. S1. Phase-behavior of single polymers in explicit solvent, insight from Molecular Dynamics computer simulations. Polymers are modeled as linear chains of beads (or monomers) and solvent molecules as single particles; monomers and solvent particles have the same linear size $= b$, and monomer-monomer (mm), solvent-solvent (ss) and monomer-solvent (ms) interactions are of the Lennard-Jones type. (a) The first set-up is from Ref. [16], with a single chain immersed in a bath of solvent molecules at density $\rho_s = 0.64/b^3$. mm and ss pair interactions are attractive, with equal fixed strength defining our energy scale ($\epsilon_{mm} = \epsilon_{ss} = -\epsilon < 0$); the ms interaction is attractive and of variable strength. The polymer mean gyration radius in bond units (R_g/b , l.h.s.) as a function of the ms strength ($-\epsilon_{ms}/\epsilon$) demonstrates that the polymer undergoes a *compact-swollen-compact* re-entrant behavior upon *increasing* the polymer affinity with the solvent. The re-entrant globule phase is characterized by the presence of solvent molecules inside the globule, which makes it more swollen. On the r.h.s., a few representative chain conformations from low to high ms affinity (panels (A) to (E)). Notice that in the same work, the authors discussed also multi-chain systems. **Reprinted and adapted from [16], with the permission of John Wiley and Sons.** (b) The second set-up is from Ref. [17], with a single chain immersed in a bath of solvent molecules at density $\rho_s = 0.047/b^3$ (*i.e.*, very dilute conditions and, so, much smaller than in the previous case). The ss interaction strength ($\epsilon_{ss} = -\epsilon$) fixes the energy scale, and mm (ϵ_{mm}) and ms (ϵ_{ms}) are varied to characterize the mean chain gyration radius (l.h.s.) and the phase diagram (r.h.s.). For relevant parameters here ($\epsilon_{mm} = \epsilon_{ss}$, bottom line in the l.h.s. panel), by increasing the ms affinity the chain undergoes a transition from two distinct compact phases, from one (CI) stabilized by intra-polymer interactions to that (CB) stabilized by bridging (solvent-mediated) interactions. **Reprinted and adapted from Ref. [17], with the permission of AIP Publishing.**

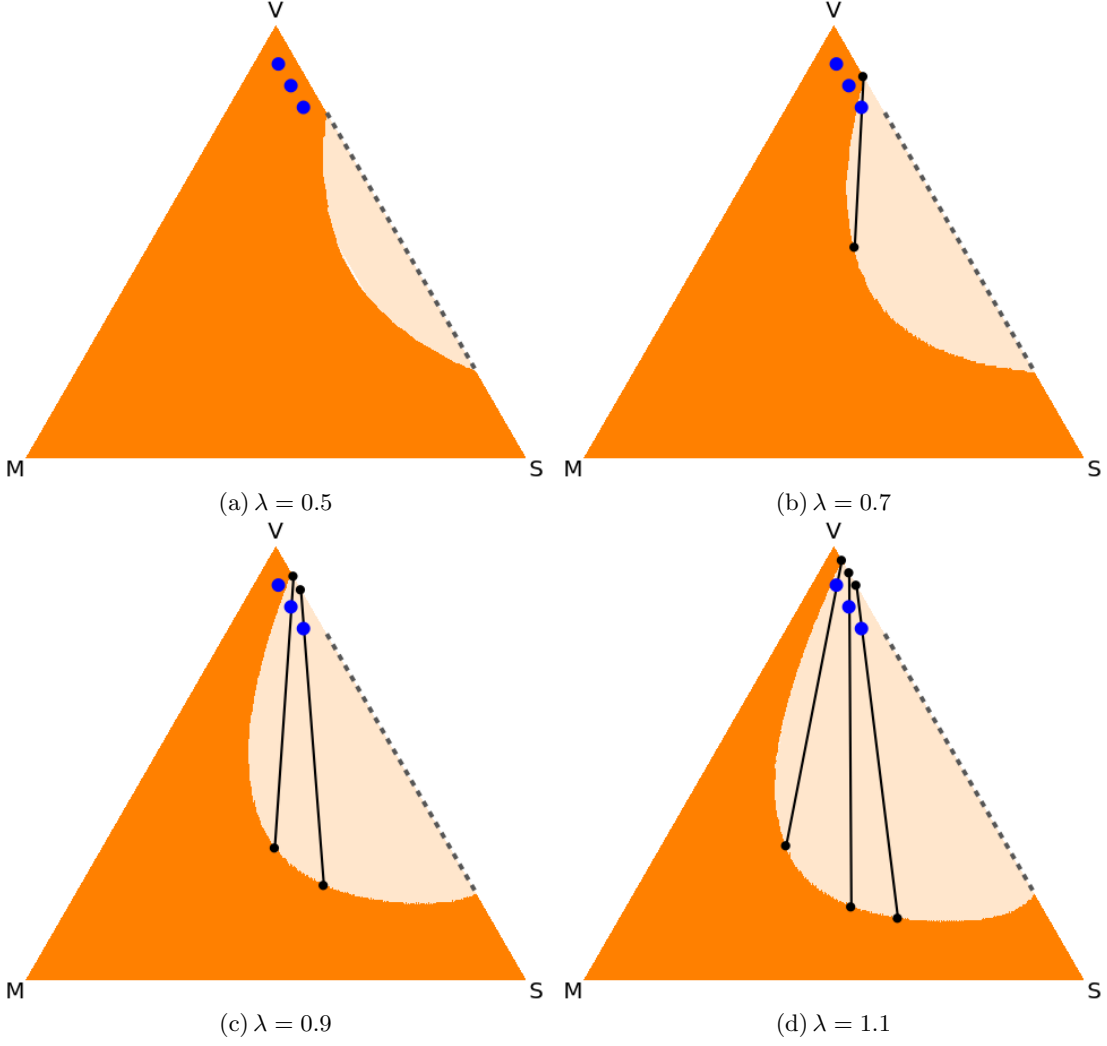


FIG. S2. Single-chain systems, polymer-assisted condensation (Eq. (2) in the main text with $d = 3$, $\epsilon_{mm} = 0$, $\epsilon_{ss} = -\epsilon < 0$, $\epsilon_{ms} = -\lambda\epsilon$ ($\lambda > 0$) and $T^* = k_B T / \epsilon = 1.3$). The gray dashed line denotes the *miscibility gap* [2] of the binary SV mixture: its extremities correspond to the binodal concentrations. The three large blue dots denote corresponding mean compositions of the system with the same monomer density $\phi_m = 0.04$ and as many values of ϕ_s outside the miscibility gap.

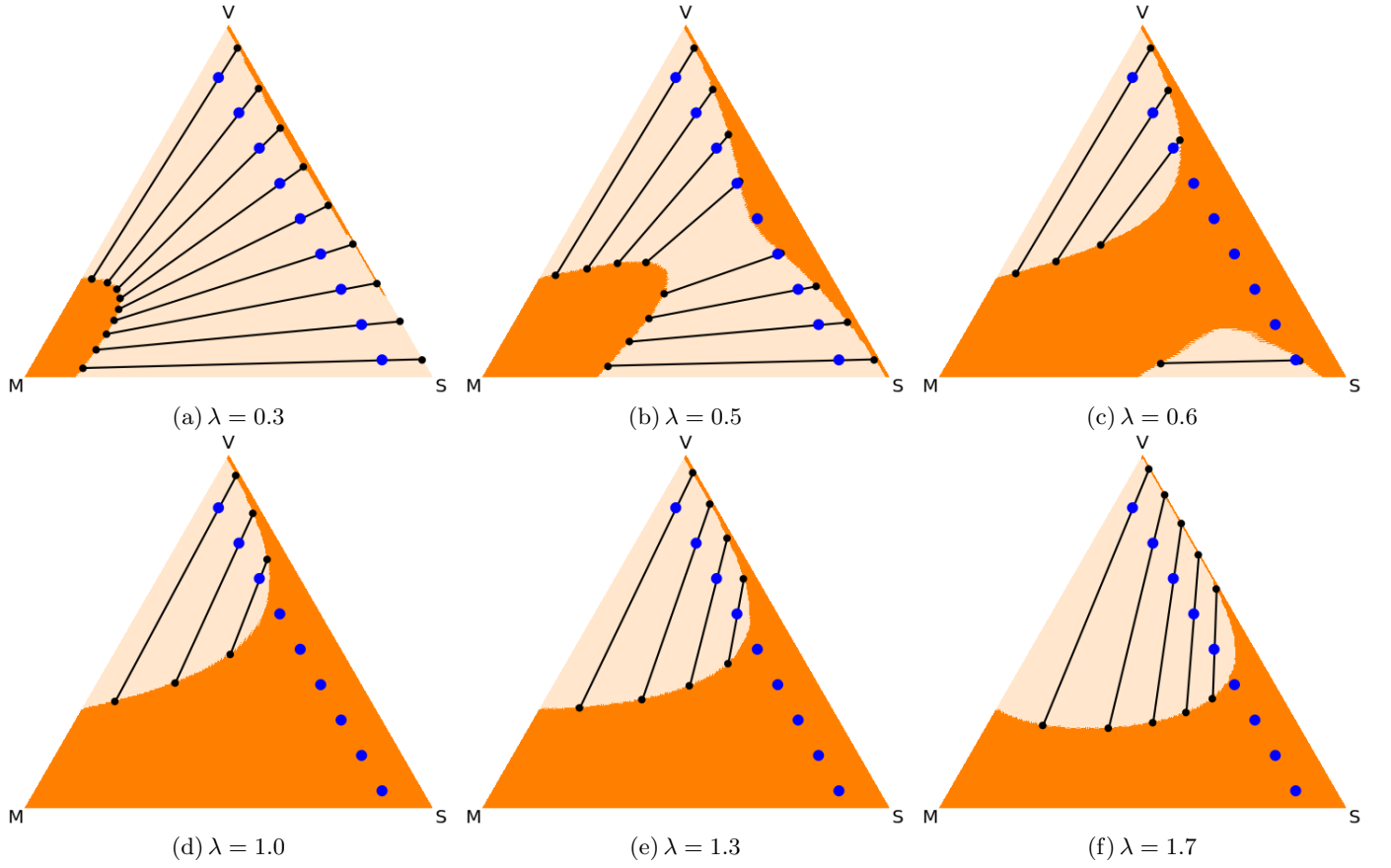


FIG. S3. Multi-chain systems, two-phase stability (Eq. (2) in the main text with d , ϵ_{mm} , ϵ_{ss} , ϵ_{ms} and T^* as in the caption of Fig. 3 in the main text, and with chains of finite mean contour length $\ell = 10$). Symbols (in particular, the blue points corresponding to 9 chosen mean compositions of the system with the same $\phi_m = 0.1$), color code and notation are as in Fig. 3 in the main text. The positions of the black dots are calculated by solving numerically Eqs. (S36)-(S39).

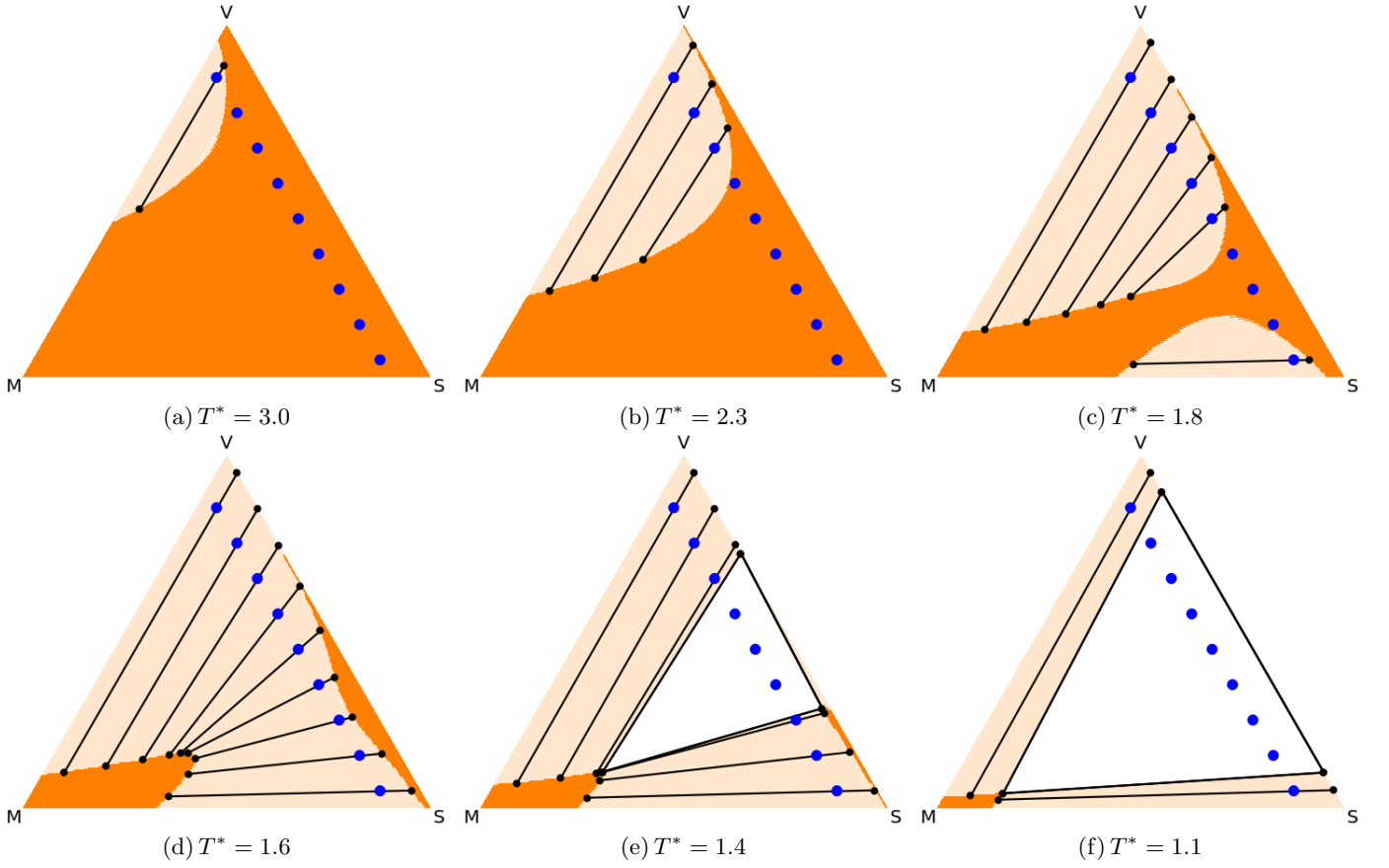


FIG. S4. Multi-chain systems, three-phase stability (Eq. (2) in the main text with d , ϵ_{mm} , ϵ_{ss} , ϵ_{ms} and T^* as in the caption of Fig. 4 in the main text, and with chains of finite mean contour length $\ell = 10$). At high temperatures (panels (a) to (c)) the behavior is similar to the single-chain situation, with larger portions of the Gibbs triangle interested by two-phase separation as temperature drops. As temperature drops below the critical value (panels (d) to (e)), the triphasic region (white triangular region) becomes stable: the system at any mean composition inside this region separates into 3 coexisting phases of compositions (obtained by solving numerically Eqs. (S40)-(S45)) lying at the corners of the white triangle. Symbols (in particular, the blue points corresponds to 9 chosen mean compositions of the system with the same $\phi_m = 0.1$), color code and notation are as in Fig. 3 in the main text.